



Available online at  
<http://ojs.unik-kediri.ac.id/index.php/ukarst/index>

 <http://dx.doi.org/10.30737/ukarst.v5i1>

**U KaRST**

## Identification of Physical and Mineralogical Properties of Riverbank Material at Sand Mining Landslide Sites of Kali Putih River, Blitar

A. M. Hapsari<sup>1\*</sup>, D. Sisinggih<sup>2\*</sup>, A. P. Hendrawan<sup>3</sup>, S. Wahyuni<sup>4</sup>

<sup>1,2\*,3,4</sup>Faculty of Engineering, Brawijaya University

E-mail: <sup>2\*</sup> [singgih@ub.ac.id](mailto:singgih@ub.ac.id)

### ARTICLE INFO

#### Article history:

Article entry : 18-09-2020

Article revised : 17-10-2020

Article received : 27-10-2020

#### Keywords:

Mineralogy, Physical Properties, Riverbank, Sand Mining.

#### IEEE Style in citing this article:

[20] R. D. Hryciw, J. Zheng, and K. Shetler, "Particle roundness and sphericity from images of assemblies by chart estimates and computer methods," *J. Geotech. Geoenvironmental Eng.*, 2016, doi: 10.1061/(ASCE)GT.1943-5606.0001485.

### ABSTRACT

Kali Putih River is a river that is often affected by the eruption of Mount Kelud. The resulting large deposits of volcanic sand materials cause exploitation through uncontrolled sand mines. This will impact potential hazards caused by environmental damage; for example, there have been several cases of riverbank landslides. Based on previous studies, it is important to study identifying physical characteristics and mineralogy of riverbank materials through laboratory testing. Found the Gs value to be within 2.650-2.697, classified as gravel or sand. According to the AASHTO standard, the classification is coarse-grained soil. By USCS classification, all samples were determined as well-graded sand. Based on the JGS standard, these samples can be classified as Volcanic Soil (VS) and Volcanic Sand (SV). SEM results showed that the grain samples had low sphericity with angular to sub-angular and a bladed-oblate granular form. From X-RD analysis, the mineral composition of samples was dominated by anorthite ( $\text{CaAl}_2\text{Si}_2\text{O}_8$ ) and albite ( $\text{Na}(\text{AlSi}_3\text{O}_8)$ ). Associated with Bowen's Reaction, these compounds are common in young materials when the weathering process is still progressing.

## 1. Introduction

Mount Kelud is one of the stratovolcanoes (conical composite volcano) that is the most active and dangerous [1]. Throughout its eruptive history, the volcano formed from accumulated lava flows, forming the stratovolcano. The height of Mount Kelud reaches 1731 masl (meters above sea level) and is located in the regencies of Kediri, Malang, and Blitar [2]. From the years 1000-2014, Mount Kelud has erupted 34 times. The last violent eruption of Mount Kelud was on February 13, 2014, when ejected pyroclastic material was to a height of 7 km [3]. Another impact of the eruption was bursts of lightning, with the greatest energies

being within 50 km from the crater, and dark clouds even extended up to a distance of 200 km against the wind, which indicated that lightning occurred in areas with the highest concentrations of particles as well as in areas with turbulence [4]. The seismic energy released before the eruption of Mount Kelud in 2014 was approximately 6 times greater than what was released before the 2007 eruption. The estimated volume of material that was ejected in the 2014 eruption ( $140\text{-}280 \times 10^6 \text{ m}^3$  dense rock equivalent-DRE) was 4 to 8 times greater than the 2007 eruption ( $35 \times 10^6 \text{ m}^3$  DRE) [5].

The outflows of bright lava, accompanied by volcanic ash and gravel plumes, caused a rain of volcanic ash in several regions, as Blitar, Kediri, Solo, Yogyakarta, Purwokerto, Cilacap, and several areas in Bandung, West Java [6]. The areas affected by the Mount Kelud eruption in Blitar Regency covered four sub-districts: Nglegok Sub-District, three villages in Garum Sub-District, and seven villages in Gandusari Sub-District [7]. One of the rivers affected by the Mount Kelud eruption was the Kali Putih River, located in Karangrejo Village in Garum Sub-District, Blitar Regency.

The volcanic material present along the banks of the Kali Putih River makes the areas around the river possess the potential to become sites for the mining of materials, specifically sand. However, the sand mining that occurs in the location is uncontrolled, which leads to the potential of over-exploitation and can lead to an increased risk of disasters, one of them being landslides.

A landslide on the banks of Kali Putih River on January 14, 2018, caused two injuries, three people to become isolated, and one mining truck to become buried. Based on the above events, a physical and mineralogical identification of material at landslide sites on the Kali Putih River becomes necessary.

## 2. Literature Review

### 2.1. Sieve Analysis

Sieve analysis is an effort to determine the distribution of soil particle sizes with the usage of a sieve [8]. Sieve analysis, or sometimes called particle gradation analysis, is a test that is performed to determine the size variations of particles present in soil with particles of diameters  $> 0.075 \text{ mm}$ . The objective of sieve analysis, among others, is to find out the condition of the gradation – whether good, poor, or uniform, as well as to find out the sizes of soil particles.

## 2.2. Specific Gravity Analysis

Specific gravity compared the mass of soil and distilled water mass at the same temperature and volume [9]. In other words, specific gravity is the comparison (ratio) between the mass of dry soil particles and that of distilled water of the same volume as the particles' volume. Specific gravity is the comparison of the mass of a volume of solid particles ( $\gamma_s$ ) to the mass of a volume of water ( $\gamma_w$ ) at a temperature of 4 °C, which can be formulated as the following:

$$G_s = \frac{\gamma_s}{\gamma_w}$$

## 2.3. Density and Void Ratio Analysis

May compose soil of two or three parts. Dry soil is only composed of two parts, which are soil particles and air pores. Soil that is fully saturated comprises the two parts, of solids or particles and water pores. In an unsaturated condition, the soil comprises three parts: solids (particles), air pores, and water pores. Can define the effective void ratio as the effective pore volume ratio to the soil particle volume [10].

## 2.4. X-RD (X-Ray Diffraction) Analysis

X-ray diffraction is performed to obtain the content of easily weathered primary minerals present in soil samples. The resulting mineral analysis is then analyzed descriptively based on a chart that indicates mineral contents [11]. Minerals are elements that occur through a natural process with certain chemical components composed of combinations of inorganic compounds and distinct crystal structures. The primary advantage of utilizing the X-RD method for material characteristics is its penetration ability because this method has very high energy due to its very short wavelengths. The XRD method has been applied in detecting mineral characteristics from volcanic eruptions on Tenerife Island [12].

## 2.5. SEM (Scanning Electron Microscope) Analysis

SEM is utilized to determine the surface morphology, surface topographic structure, particle sizes, structural deficiencies, and impurity composition of a material. SEM has a magnification of 10–3,000,000 kali, depth of field of 4–0.4 mm, and resolution of 1–10 nm. The obtained results are presented in three-dimensional form as pictures or photos. Previous researchers have carried out the application of SEM in several fields of science: SEM as a tool

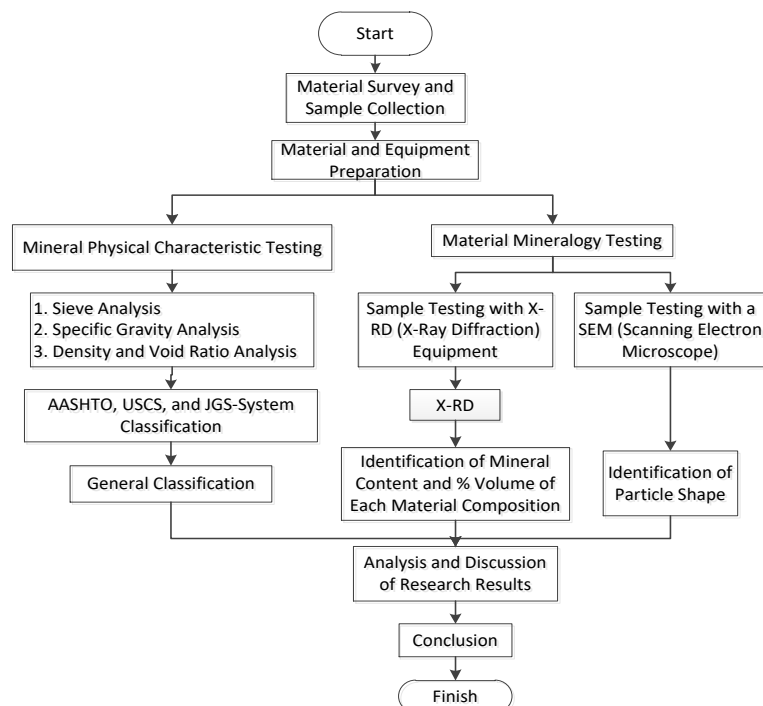
to prove the evidence of repeated forest fires from Permian coal deposits [13] and nano-scale 2D SEM for reconstructing 3D pore system [14].

## 2.6. Sphericity and Roundness

The degree of sphericity (ball quality) and the degree of roundness (circularity) is utilized to classify and find out the morphology of soil in the fields of engineering and geology [15]. Sphericity is determined by comparing the surface area of the particle with the volume of a ball. In contrast, roundness is determined by the particle's arc angles [15][16]. The shapes of these particles depend on the structure type and mineralogical composition of the rock. Transport of rocks, temperature, and moisture does not significantly affect particle form changes [17].

## 3. Research Method

Conducted this research by utilizing soil samples from several landslide sites of the Kali Putih River banks. There were four sites for sample collection and composed each site of 3 points. The research flowchart explains the process in more detail (Figure 1).



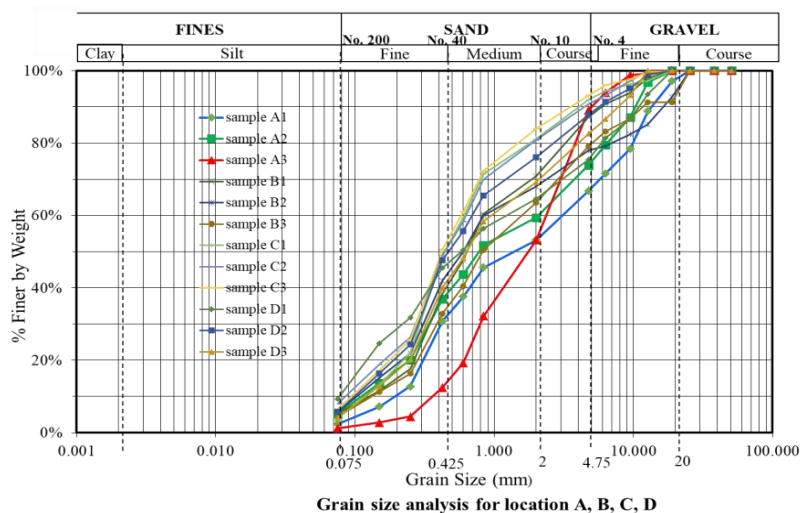
Source : Research Flowchart, 2020

**Figure 1.** Research Flowchart

### 4. Results and Discussion

#### 4.1. Sieve Analysis

Sieve analysis or soil gradation analysis was performed to find out the variations in particle size by sifting with the standard sieve of ASTM (American Standard Testing Materials). This analysis is intended to highlight information regarding variations. The sifting process determines the variations of soil particle sizes with the standard ASTM sieve. The variations in size are then displayed as a distribution curve of particle gradations as in Figure 2.



Source : Analysis Results, 2019

**Figure 2.** Particle Distribution Curve at the Study Sites

The distribution of particle gradations in Figure 2 showed that the particle gradation in a range of fines to fine gravel. According to the particle gradation distribution, the particle size can be read for each sampling point, and the results are outlined in Table 1.

**Tabel 1.** Summary of Particle Gradations at the Study Sites

Sample Point	Fines (%) (< 0.075) (mm)	Fine sand (%) (0.425 – 0.075) (mm)	Medium sand (%) (2 – 0.425) (mm)	Coarse sand (%) (4.75 – 2) (mm)	Fine gravel (%) (20 – 4.75) (mm)	Coarse gravel (%) (100 – 20) (mm)
A1	2.40	28.40	22.40	13.60	33.20	0.00
A2	5.22	31.73	22.49	14.46	26.10	0.00
A3	1.21	11.29	40.73	35.89	10.89	0.00
B1	5.20	33.20	32.40	16.40	12.80	0.00
B2	5.60	36.40	26.00	10.00	22.00	0.00
B3	4.40	28.40	30.80	15.60	20.80	0.00
C1	4.02	44.98	32.13	10.84	8.03	0.00

Sample Point	Fines (%) ( $< 0.075$ ) (mm)	Fine sand (%) ( $0.425 - 0.075$ ) (mm)	Medium sand (%) ( $2 - 0.425$ ) (mm)	Coarse sand (%) ( $4.75 - 2$ ) (mm)	Fine gravel (%) ( $20 - 4.75$ ) (mm)	Coarse gravel (%) ( $100 - 20$ ) (mm)
C2	8.00	40.80	32.00	10.00	9.20	0.00
C3	6.43	44.18	33.33	9.24	6.83	0.00
D1	9.27	36.29	18.95	10.89	24.60	0.00
D2	5.69	41.87	28.46	11.79	12.20	0.00
D3	4.05	36.03	29.15	13.36	17.41	0.00

Source : Analysis Results, 2019

Table 1 shows that the particle gradation at the study sites is dominated by fine sand, but there is no gravel. The results of the summary of particle gradations, classification was then performed based on percentages of particle diameters by calculating the values of uniformity coefficient (Cu) and gradation coefficient (Cc). The following is the classification based on the values of Cu and Cc, according to Das (1995):

**Table 2.** Gradation Classification of Particles at the Study Sites

Site	Sample Point	D <sub>10</sub>	D <sub>30</sub>	D <sub>60</sub>	Cu	Cc	Gradation Classification
A	A1	0.200	0.430	3.200	16.000	0.289	Fair
	A2	0.110	0.350	2.000	18.182	0.557	Fair
	A3	0.370	0.800	2.400	6.486	0.721	Fair
B	B1	0.140	0.350	0.850	6.071	1.029	Good
	B2	0.110	0.300	0.850	7.727	0.963	Fair
	B3	0.140	0.400	1.800	12.857	0.635	Fair
C	C1	0.120	0.300	0.600	5.000	1.250	Fair
	C2	0.080	0.280	0.610	7.625	1.607	Good
	C3	0.094	0.290	0.600	6.383	1.491	Good
D	D1	0.073	0.230	1.400	19.178	0.518	Fair
	D2	0.100	0.280	0.700	7.000	1.120	Good
	D3	0.130	0.320	0.970	7.462	0.812	Fair

Source : Research Results, 2019

The gradation classification based on Cu and Cc values was obtained in a fair and good gradation classification.

#### 4.2. Specific Gravity Analysis

Specific gravity is the comparison of the mass of a volume of solid particles ( $\gamma_s$ ) toward the mass of a volume of water ( $\gamma_w$ ) at the temperature of 4 °C, as Equation in bellow:

$$G_s = \frac{\gamma_s}{\gamma_w}$$

$\gamma_s$  = mass of a volume of solids

$\gamma_w$  = mass of a volume air

The results of specific gravity analysis for the samples in the study refer to Table 2, and the following are the results of the classification in Table 3:

**Table 3.** Results of Specific Gravity Analysis for Samples

Site Point	Sample	Gs Value	Soil Type
A	A1	2.677	Gravel/Sand
	A2	2.691	Gravel/Sand
	A3	2.657	Gravel/Sand
B	B1	2.672	Gravel/Sand
	B2	2.683	Gravel/Sand
	B3	2.652	Gravel/Sand
C	C1	2.67	Gravel/Sand
	C2	2.662	Gravel/Sand
	C3	2.650	Gravel/Sand
D	D1	2.664	Gravel/Sand
	D2	2.653	Gravel/Sand
	D3	2.697	Gravel/Sand

Source : *Research Results, 2019*

The Gs Value based on specific gravity analysis results is 2.650 to 2.697, which can be classified as gravel or sand.

#### 4.3. Density and Void Ratio Analysis

This analysis was performed by comparing the number of soil pores in the loosest condition and soil condition on the field to compare the number of soil pores in the loosest and most packed conditions. The objective was to find out the mass, relative density, number of pores, and porosity of each sample analyzed. Results of  $e_{\max}$  and  $e_{\min}$  for the study results indicated that the type of soil from the analyzed samples is considered clean sandy soil with an  $e_{\min}$  value of 0.38-0.61 and an  $e_{\max}$  value of 0.66-0.86. For more details, it will be shown in Table 4:

**Table 4.** Results of  $e_{\max}$  and  $e_{\min}$  value for Samples

Site Point	Ws Loose gr	Ws Dense gr	$\gamma_d$ min gr/cm <sup>3</sup>	$\gamma_d$ max gr/cm <sup>3</sup>	Gs	$e_{\min}$	$e_{\max}$
A1	702	830	1.489	1.761	2.677	0.520	0.798
A2	681	831	1.445	1.763	2.691	0.526	0.863
A3	692	780	1.468	1.655	2.657	0.606	0.810
B1	688	844	1.460	1.790	2.672	0.492	0.831
B2	672	798	1.426	1.693	2.683	0.585	0.882
B3	700	860	1.485	1.824	2.652	0.454	0.786
C1	738	858	1.566	1.820	2.67	0.467	0.705
C2	682	822	1.447	1.744	2.66	0.525	0.839
C3	680	794	1.443	1.684	2.65	0.573	0.837

Site Point	Ws Loose gr	Ws Dense gr	$\gamma_d$ min gr/cm <sup>3</sup>	$\gamma_d$ max gr/cm <sup>3</sup>	Gs	$e_{min}$	$e_{max}$
D1	696	834	1.476	1.769	2.664	0.506	0.804
D2	750	904	1.591	1.918	2.653	0.383	0.667
D3	710	854	1.506	1.812	2.679	0.479	0.779

Source : *Research Results, 2019.*

#### 4.4. Sphericity and Roundness

Figure 3 shows the example of particle length measurement for a sample by utilizing SEM results. The results of the above measurement were utilized to determine the value of shape factor (F) and shape, according to Zingg (1935) with Equation in bellow [18]:

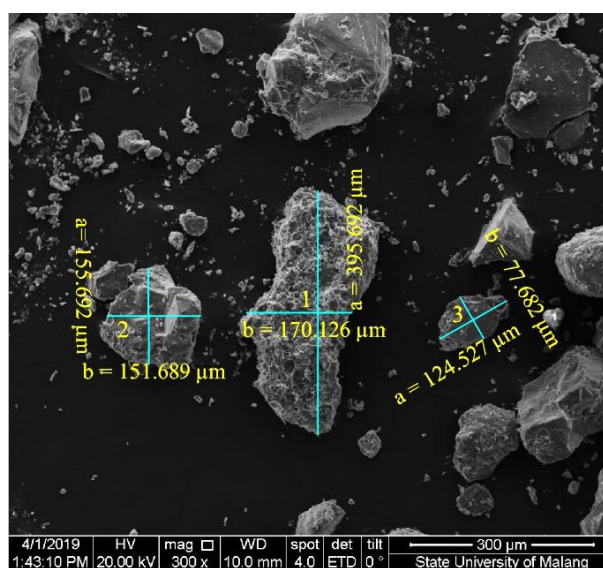
$$F = \frac{c}{\sqrt{a \cdot b}}$$

Where:

a = longest axis

b = medium axis

c = shortest axis (0.5 b)



Source : *Research Results, 2019*

**Figure 3.** Results of Sample A2 Measurement

Table 5 shows the results for the performed calculations for the Shape Factor value.

**Table 5.** Shape Factor Value and Particle Shape

No	a (μm)	b (μm)	c (μm)	F	b/a	c/b	Remarks
Sample A2							
A2 (1)	395.692	170.126	85.063	0.328	0.430	0.500	<i>Bladed</i>
A2 (2)	155.692	151.689	75.845	0.494	0.974	0.500	<i>Oblate</i>
A2 (3)	124.527	77.682	38.841	0.395	0.624	0.500	<i>Oblate</i>
Sample B3							
B3 (1)	205.063	148.803	74.401	0.426	0.726	0.500	<i>Oblate</i>
B3 (2)	295.735	154.183	77.091	0.361	0.521	0.500	<i>Bladed</i>
B3 (3)	192.695	175.243	87.622	0.477	0.909	0.500	<i>Oblate</i>
Sample C1							
C1 (1)	311.318	190.826	95.413	0.391	0.613	0.500	<i>Bladed</i>
C1 (2)	196.665	167.075	83.537	0.461	0.850	0.500	<i>Oblate</i>
C1 (3)	212.706	178.983	89.492	0.459	0.841	0.500	<i>Oblate</i>
Sample C2							
C2 (1)	553.975	236.260	118.130	0.327	0.426	0.500	<i>Bladed</i>
C2 (2)	250.891	138.436	69.218	0.371	0.552	0.500	<i>Bladed</i>
C2 (3)	208.737	167.993	83.997	0.449	0.805	0.500	<i>Oblate</i>
Sample D1							
D1 (1)	351.044	187.184	93.592	0.365	0.533	0.500	<i>Bladed</i>
D1 (2)	377.551	222.974	111.487	0.384	0.591	0.500	<i>Bladed</i>
D1 (3)	235.407	193.614	96.807	0.453	0.822	0.500	<i>Oblate</i>

Source : *Research Results, 2019*

The roundness value is obtained by measuring the radii of arc angles for each particle. More detailed measurements of angle radii lead to obtained results that more specifically represent the shape of the particles from the samples. The roundness value is

calculated by Equation in bellow [19] [20]:

$$\text{Roundness} = \frac{\sum_{i=1}^n \left(\frac{r_i}{R}\right)}{n}$$

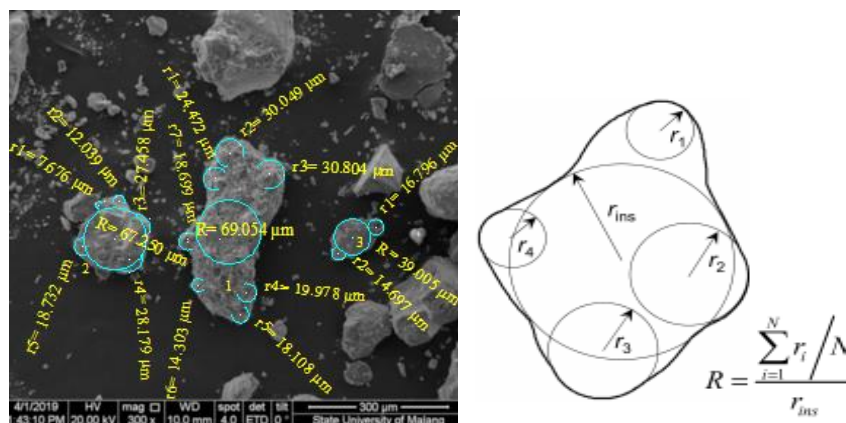
Where:

R = largest radius of the particle

ri = arc angle radii

n = number of measured arc angle radii

Figure 4 shows the results of measuring arc angle radii for Sample A2.



Source : *Research Results, 2019*

**Figure 4.** Measurement of Angle Arc Radii

Results of measurement of sphericity and roundness refer to Table 5, with the F value being for sphericity and the roundness value being obtained from the measurement results as in Figure 4. The results of measurement are presented in Table 6 below:

**Table 6.** Summary of Sphericity and Roundness Values and Particle Shape

Sample	Sphericity	Roundness	Remarks
A2			
1	0.3	0.3	<i>Low Sphericity-Angular (Bladed-Oblate)</i>
2	0.5	0.3	<i>Low Sphericity-Sub Angular (Bladed-Oblate)</i>
3	0.4	0.4	<i>Low Sphericity-Sub Angular (Bladed-Oblate)</i>
B3			
1	0.4	0.5	<i>Low Sphericity-Sub Angular (Bladed-Oblate)</i>
2	0.4	0.3	<i>Low Sphericity-Angular (Bladed-Oblate)</i>
3	0.5	0.2	<i>Low Sphericity- Very Angular (Bladed-Oblate)</i>
C1			
1	0.4	0.5	<i>Low Sphericity-Sub Angular (Bladed-Oblate)</i>
2	0.5	0.3	<i>Low Sphericity-Sub Angular (Bladed-Oblate)</i>
3	0.5	0.2	<i>Low Sphericity-Very Angular (Bladed-Oblate)</i>
C2			
1	0.3	0.5	<i>Low Sphericity-Sub Rounded (Bladed-Oblate)</i>
2	0.4	0.4	<i>Low Sphericity-Sub Angular (Bladed-Oblate)</i>
3	0.4	0.3	<i>Low Sphericity-Angular (Bladed-Oblate)</i>
D1			
1	0.4	0.3	<i>Low Sphericity-Angular (Bladed-Oblate)</i>
2	0.4	0.3	<i>Low Sphericity-Angular (Bladed-Oblate)</i>
3	0.5	0.3	<i>Low Sphericity-Sub Angular (Bladed-Oblate)</i>

Source : *Research Results 2019*

#### 4.5. AASHTO Classification

Results of classification with the AASHTO (American Association of State Highway and Transportation Officials) system indicated that all the soil samples that were tested were of the coarse-grained soil group, symbolized as A-1b. The tested soil samples were included in the general classification of soil with coarse grain, not fine soil with silt or clay. It was found that 35% or less of the soil sample passed through the No. 200 sieves. The most dominant type of material was gravel and sand, with the evaluation as base soil material being very good to good.

#### 4.6. USCS Classification

Based on the classification results with the USCS (Unified Soil Classification System), all the soil samples at the study sites were of the sandy well-graded soil type, containing sandy gravel with some fine particles, symbolized as SW (Well-graded Sand). The research results found that the percentage of materials that passed the No. 4 sieve was greater than 50%, with 17% being of gravel size and 83% of the sand size.

#### 4.7. JGS Classification

The JGS (Japanese Geotechnical Society) classification is based on the percentage of the samples that passed the No. 200 sieves. Based on the study results that were performed on the samples, the value of  $F_c$  was found to be less than 50%; the test samples were classified as volcanic soil and volcanic sand with coarse-grained soil.

**Table 7.** Results of Soil Sample Classification with the JGS Method

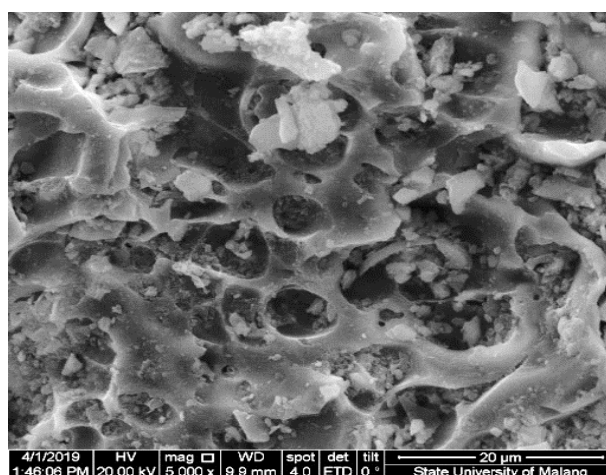
Sample	% Passed Sieve No. 200	Symbol
A1	2.40%	V
A2	5.22%	S-V
A3	1.21%	V
B1	5.20%	S-V
B2	5.60%	S-V
B3	4.40%	V
C1	4.02%	V
C2	8.00%	S-V
C3	6.43%	S-V
D1	9.27%	S-V
D2	5.69%	S-V
D3	4.05%	V

Source : *Research Results, 2019*

Considering its utility, volcanic soil has very good physical characteristics and is therefore of great interest because of its high content of phosphates and several other micronutrients, making it the most fertile kind of soil in the world. However, if rain occurs with high intensity, this may increase pressure to the soil pores and reduce soil strength, which can lead to slope instability.

#### 4.8. SEM (Scanning Electron Microscope) Analysis

SEM analysis was only performed on five samples out of the total of 12 available samples. This was based on the most significant differences in color and texture out of all the samples. The samples for which mineralogy analysis was performed were A2, B3, C1, C2, and D1. Below is the result of SEM analysis for the A2 sample at 5000x magnification.



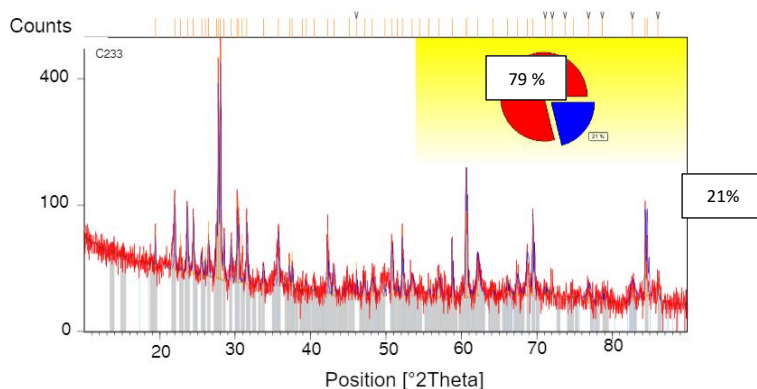
Source : *Research Results, 2019*

**Figure 5.** Results of SEM Analysis

Based on the results of SEM analysis that had been performed, cavities were found on the particles' surface. A similar result was also found for the C1, C2, and D1 samples. However, for the B3 sample, there were fewer cavities on the sample particles compared to the other samples. SEM analysis results are strongly related to the pore value results, which had a high value of 0.882.

#### 4.9. X-RD (X-Ray Diffraction) Analysis

As with SEM analysis, X-RD was only performed on five samples out of the total of 12 available samples. The results of X-RD analysis are presented in Figure 6 and Table 8.



Source : Research Results, 2019

**Figure 6.** Results of X-RD Analysis for the A2 Sample

The X-RD results obtained that the maximum peak is 512.32 and 458.91 counts, which are at the position in 28.028 and 27.753. The mineral composition of the sample was dominated by 79% anorthite and 21% albite.

**Table 8.** Mineral Content of Samples

Sample	Mineral	
	Anorthite	Albite
A2	+++	+
B3	+++	+
C1	+++	+
C2	+++	+
D1	+++	+

Source : Research Results, 2019

Legend:

- : None (0%)
- + : Little (0% - 35%)
- ++ : Moderate (35% - 70%)
- +++ : Dominant (>70%)

Results of X-RD analysis indicated that the mineral content of the samples is dominated by anorthite ( $\text{CaAl}_2\text{Si}_2\text{O}_8$ ) and albite ( $\text{Na(AlSi}_3\text{O}_8)$ ). Anorthite and albite are soils that are formed from volcanic parent material with easily weathered primary mineral content. In the Bowen Reaction, anorthite and albite are considered minerals in early weathering stages, indicating that the soil is young or has not experienced further weathering.

#### 4.10. Material Potential Based on Study Results

The study sites' materials constitute soil with good gradation, low gravel content,

more than 50% of particles passed through the No. 4 sieves and more than 95% of particles were held by the No. 200 sieves. Materials with the above characteristics are suitable for use as refill material in Class II embedded pipe, which consists of coarse sand and gravel with a maximum particle size of 40 mm, has varying gradations with little presence of fine-grained material, and is generally speckled and not well cohesive. In wet or dry conditions. In addition, based on the SEM and pore value analysis that has been performed, the material contains many air cavities and has a large pore value. Therefore, the study sites' materials are judged to be able to let water pass through the air in drainage channels.

## 5. Conclusion and Suggestions

### 5.1. Conclusion

Based on the results and discussion above, the following are the conclusions:

1. The riverbank material at landslide locations constitutes material with good gradation in sand or gravel for physical characteristics. Based on USCS and AASHTO classification, the material constitutes sandy soil with gravel and good subgrade without a plastic nature and is of the Well-Graded Sand category. Based on JGS system classification, the study sites' samples constitute soil of Volcanic Soil and Volcanic Sand types.
2. For mineral characteristics, SEM (Scanning Electron Microscope) analysis indicated that the material samples contain air cavities, have low sphericity with a bladed-oblate grain shape and have grains of angular-sub angular category. Meanwhile, the results of X-RD analysis indicate a mineral content dominated by young minerals (in the early weathering process) in the form of anorthite ( $\text{Ca}(\text{Al}_2\text{Si}_2\text{O}_8)$ ) and albite ( $\text{Na}(\text{AlSi}_3\text{O}_8)$ ).
3. The material that is present at the locations has the potential to be made into backfill material in an embedded pipe. Also, because the material possesses many air cavities of a large size, it may be perused as a layer in drainage channels.

### 5.2. Suggestions

Some suggestions can be made for further development of this research is External aspects of the material at the locations need to be considered to determine the more specific factors that cause landslides. Cemented sand characteristics in landslide material need to be investigated, along with their effects on the risk of riverbanks' landslides.

## References

- [1] F. Maeno *et al.*, “A sequence of a plinian eruption preceded by dome destruction at Kelud volcano, Indonesia, on February 13, 2014, revealed from tephra fallout and pyroclastic density current deposits,” *J. Volcanol. Geotherm. Res.*, vol. 382, pp. 24–41, 2019, doi: 10.1016/j.jvolgeores.2017.03.002.
- [2] D. Kiswiranti, “Temporal Statistical Analysis of Eruptions of Mount Kelud, Mount Semeru, and Mount Merapi,” *Tek. Geol.*, pp. 1–10, 2013.
- [3] F. Aristantha, A. P. Hendrawan, and R. Asmaranto, “Identification of The Physical and Mineralogical Characteristics of The Pyroclastic Material From The Eruption of Mount Kelud in The Kali Sambong River, Pandansari Village, Ngantang District, Malang Regency As An Alternative To The Embankment Material,” *J. Mhs. Jur. Tek. Pengair.*, vol. 1, no. 1, p. 18, 2017.
- [4] K. A. Hargie, A. R. Van Eaton, L. G. Mastin, R. H. Holzworth, J. W. Ewert, and M. Pavolonis, “Globally detected volcanic lightning and umbrella dynamics during the 2014 eruption of Kelud, Indonesia,” *J. Volcanol. Geotherm. Res.*, vol. 382, pp. 81–91, 2019, doi: 10.1016/j.jvolgeores.2018.10.016.
- [5] H. Nakamichi, M. Iguchi, H. Triastuty, M. Hendrasto, and I. Mulyana, “Differences of precursory seismic energy release for the 2007 effusive dome-forming and 2014 Plinian eruptions at Kelud volcano, Indonesia,” *J. Volcanol. Geotherm. Res.*, vol. 382, pp. 68–80, 2019, doi: 10.1016/j.jvolgeores.2017.08.004.
- [6] Purwanto and M. S. Kistiyanto, “The Spatio-Temporal Dynamics of the Impact of the Mount Kelud Eruption in Kediri Regency,” *J. Pendidik. Geogr.*, 2017, doi: 10.17977/um017v22i12017p060.
- [7] A. K. Anam, S. Winarni, and S. R. Andriani, “The Role of Volunteers in Mount Kelud Eruption Disaster Management,” *J. Inf. Kesehat. Indones.*, vol. 3, no. 1, p. 1, 2017, doi: 10.31290/jiki.v(3)i(1)y(2017).page:1-7.
- [8] National Standardization Agency, *Soil Size Analysis Test Method, SNI 3423:2008*. 2008, pp. 1–33.
- [9] National Standardization Agency, *Soil Density Test Method, SNI 1964: 2008*. 2008.
- [10] B. Hong, X. Li, L. Wang, L. Li, Q. Xue, and J. Meng, “Using the effective void ratio and specific surface area in the Kozeny-Carman equation to predict the hydraulic conductivity of loess,” *Water (Switzerland)*, vol. 12, no. 1, 2020, doi: 10.3390/w12010024.

- [11] L. Noer Aini, M. Mulyono, and E. Hanudin, “Weatherable Minerals of Merapi Pyroclastic Materials and Their Potential Benefits for Plants,” *Planta Trop. J. Agro Sci.*, vol. 4, no. 2, pp. 84–94, 2016, doi: 10.18196/pt.2016.060.84-94.
- [12] E. A. Lalla *et al.*, “Raman-IR vibrational and XRD characterization of ancient and modern mineralogy from volcanic eruption in Tenerife Island: Implication for Mars,” *Geosci. Front.*, vol. 7, no. 4, pp. 673–681, 2016, doi: 10.1016/j.gsf.2015.07.009.
- [13] S. Murthy, V. A. Mendhe, P. S. Kavali, and V. P. Singh, “Evidence of recurrent wildfire from the Permian coal deposits of India: Petrographic, scanning electron microscopic and palynological analyses of fossil charcoal,” *Palaeoworld*, vol. 00, pp. 1–14, 2020, doi: 10.1016/j.palwor.2020.03.004.
- [14] J. Guo *et al.*, “An optimized approach using cryofixation for high-resolution 3D analysis by FIB-SEM,” *J. Struct. Biol.*, vol. 212, no. 1, p. 107600, 2020, doi: 10.1016/j.jsb.2020.107600.
- [15] B. Zhou, J. Wang, and H. Wang, “Three-dimensional sphericity, roundness and fractal dimension of sand particles,” *Geotechnique*, 2018, doi: 10.1680/jgeot.16.P.207.
- [16] Y. Hayakawa and T. Oguchi, “Evaluation of gravel sphericity and roundness based on surface-area measurement with a laser scanner,” *Comput. Geosci.*, 2005, doi: 10.1016/j.cageo.2005.01.004.
- [17] J. M. Rodriguez, T. Edeskär, and S. Knutsson, “Particle shape quantities and measurement techniques-A review,” *Electron. J. Geotech. Eng.*, vol. 18 A, pp. 169–198, 2013.
- [18] M. A. Maroof, A. Mahboubi, A. Noorzad, and Y. Safi, “A new approach to particle shape classification of granular materials,” *Transp. Geotech.*, vol. 22, p. 100296, 2020, doi: 10.1016/j.trgeo.2019.100296.
- [19] I. Cruz-Matías *et al.*, “Sphericity and roundness computation for particles using the extreme vertices model,” *J. Comput. Sci.*, vol. 30, pp. 28–40, 2019, doi: 10.1016/j.jocs.2018.11.005.
- [20] R. D. Hryciw, J. Zheng, and K. Shetler, “Particle roundness and sphericity from images of assemblies by chart estimates and computer methods,” *J. Geotech. Geoenvironmental Eng.*, 2016, doi: 10.1061/(ASCE)GT.1943-5606.0001485.